Supplemental Document

Optics EXPRESS

HyperColorization: propagating spatially sparse noisy spectral clues for reconstructing hyperspectral images: supplement

M. Kerem Aydin,[1] Qi Guo,[2] and Emma Alexander[1,*]

[1] *Department of Computer Science, McCormick School of Engineering and Applied Science, Northwestern University, 2233 Tech Drive, Evanston, Illinois 60208, USA*
[2] *Elmore Family School of Electrical and Computer Engineering, Purdue University, 501 Northwestern Avenue, West Lafayette, Indiana 47907, USA*
[*] *ealexander@northwestern.edu*

Supplement DOI: https://doi.org/10.6084/m9.figshare.25232929

Parent Article DOI: https://doi.org/10.1364/OE.508017

HyperColorization: Propagating spatially sparse noisy spectral clues over hyperspectral images: supplemental document

HyperColorization Rank and Exposure Time: Additional Examples

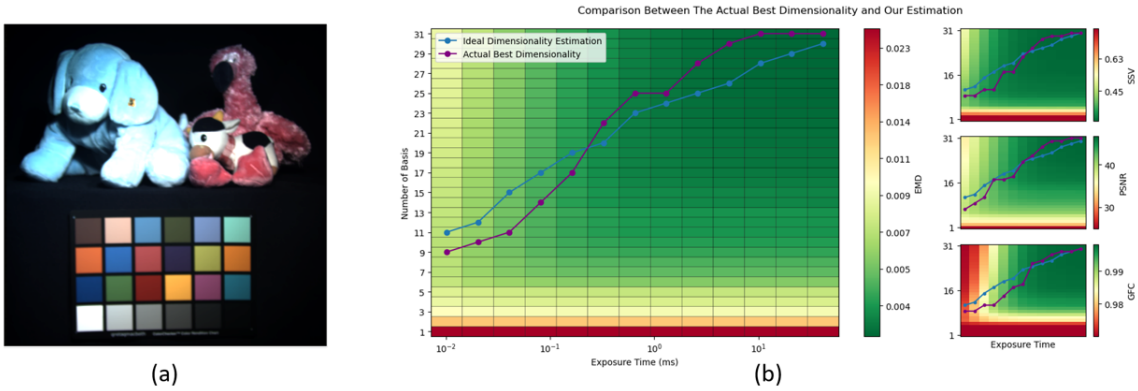

Figure S1. Image from CAVE dataset [1], brightness boosted by 20%. (b) How the optimal and estimated colorization dimensionality varies with exposure time for image in (a).

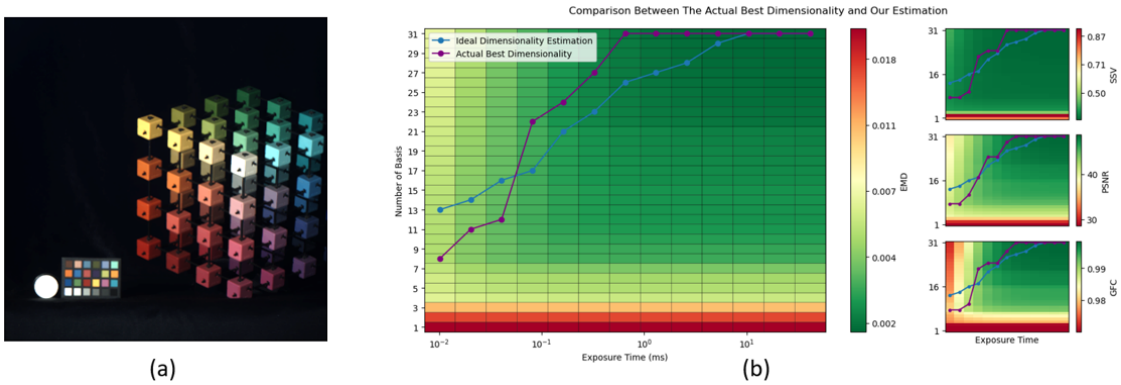

Figure S2 Image from KAIST dataset [4], brightness boosted by 40%. (b) How the optimal and estimated colorization dimensionality varies with exposure time for image in (a).

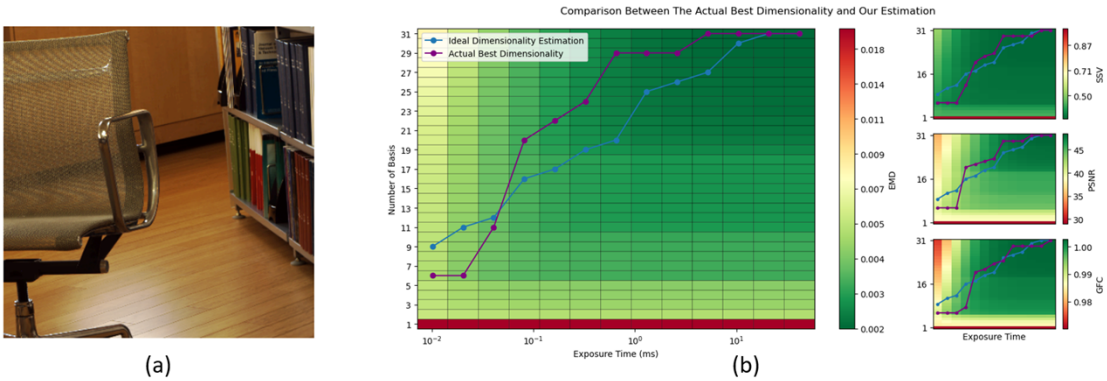

Figure S3 Image from Harvard dataset [2], brightness boosted by 65%. (b) How the optimal and estimated colorization dimensionality varies with exposure time for image in (a).

Sampling Patterns: Additional Examples

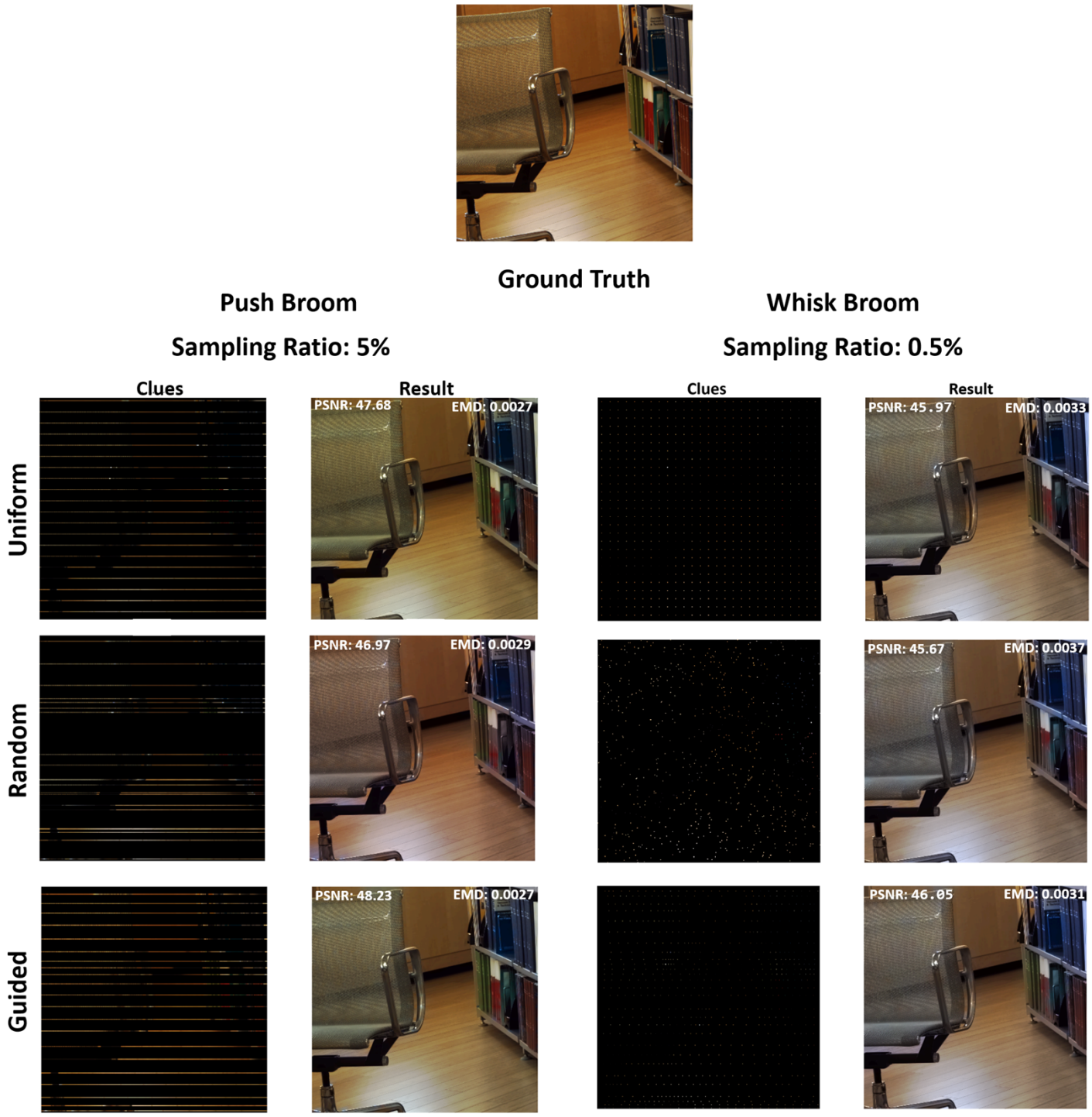

Figure S4. Brightness if boosted by 65% and size of spectral clues increased. Image from the Harvard dataset [2].

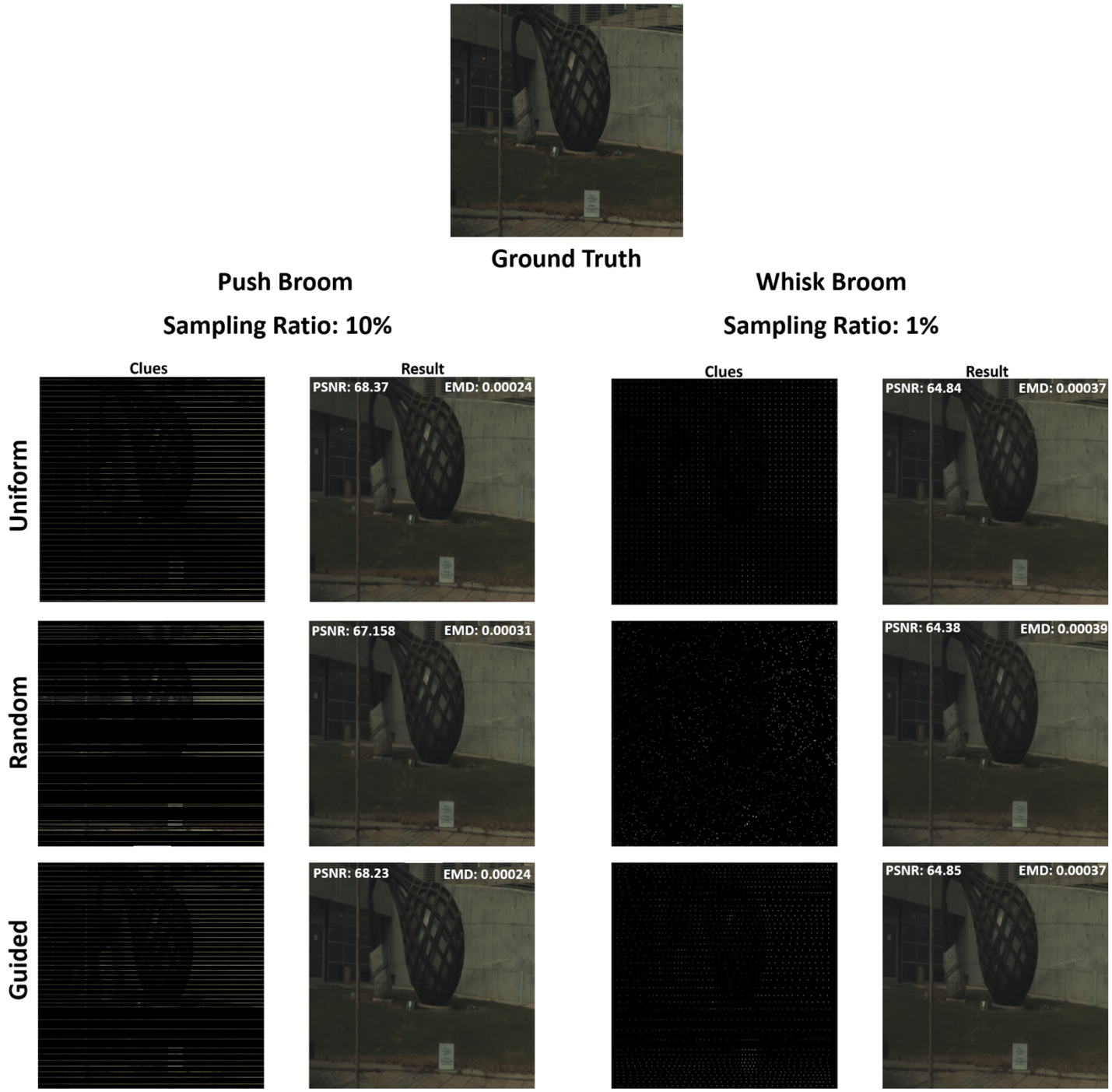

Figure S5. Brightness boosted by 30% and size of spectral clues increased. Image from the ICVL dataset [3] which features 512 channels.

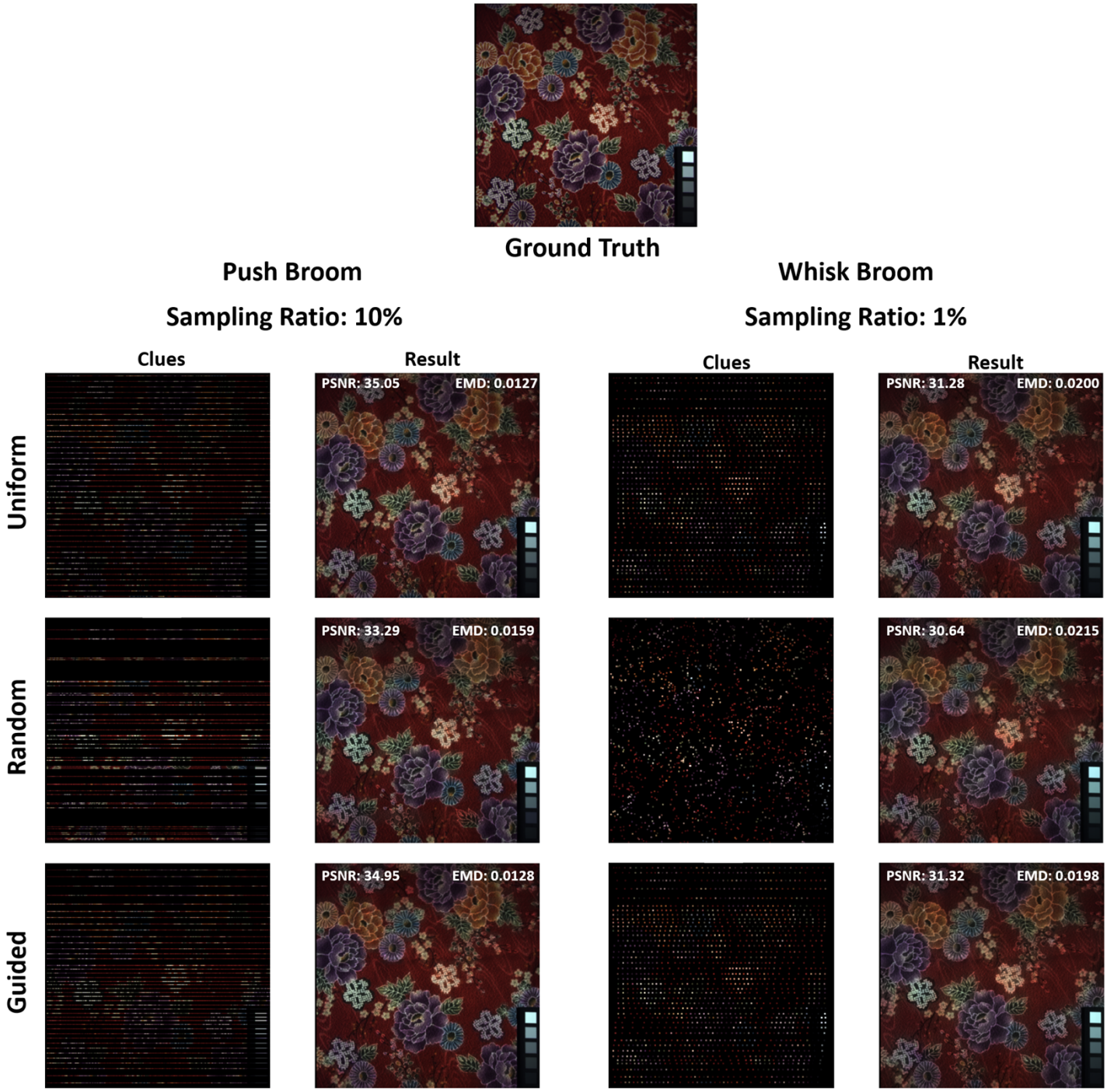

Figure S6. Brightness boosted by 40% and size of spectral clues increased. Image from the CAVE dataset [1] where guided sampling is outperformed by uniform sampling.

Imaging with a Fixed Time Budget: Additional Examples

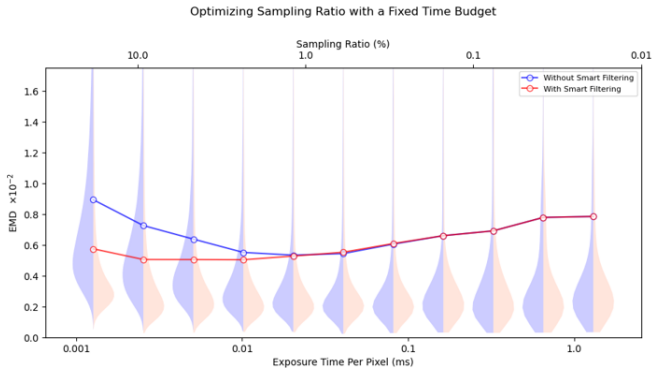

(a) (b)

Figure S7 (a) Image from Harvard dataset [2], brightness boosted by 70%. (b) The trade-off between sampling ratio and exposure time when smart filter is enabled and disabled on image (a).

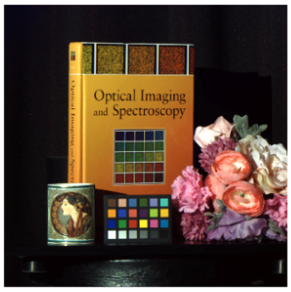

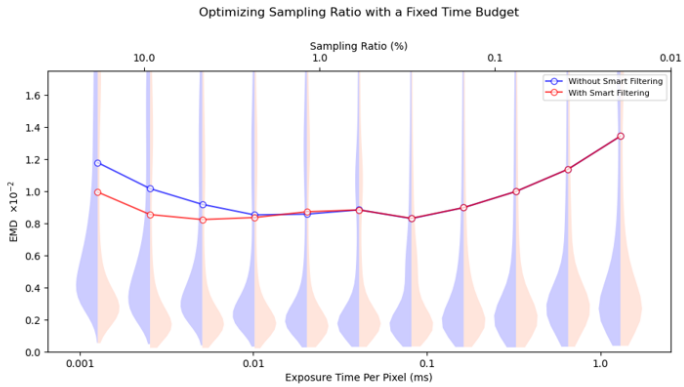

(a) (b)

Figure S8 (a) Image from KAIST dataset [4], brightness boosted by 50%. (b) The trade-off between sampling ratio and exposure time when smart filter is enabled and disabled on image (a).

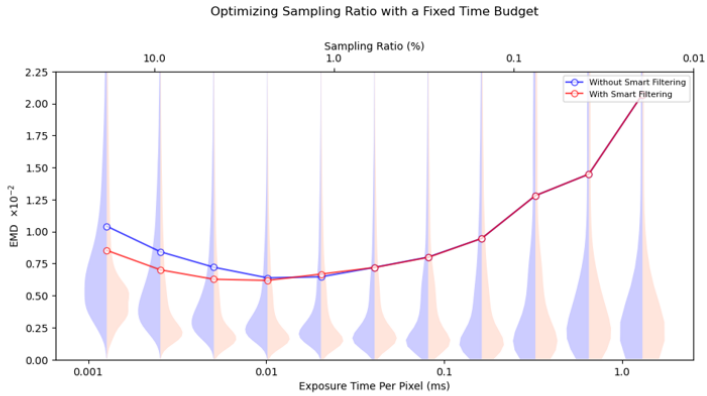

(a) (b)

Figure S9 (a) Image from CAVE dataset [1], brightness boosted by 60%. (b) The trade-off between sampling ratio and exposure time when smart filter is enabled and disabled on image (a).

Table S1. Sampling Patterns Performance Analysis on Harvard dataset

Sampling Type	Sampling Ratio	PSNR↑	SSV↓	GFC↑	EMD ↓ 10^{-3}
Uniform push broom	10%	37.938	0.342	0.992	6.865
Uniform push broom	4%	35.155	0.433	0.989	9.340
Guided push broom	4%	35.500	0.409	0.989	9.261
Uniform whisk broom	4%	37.895	0.358	0.992	6.789
Guided whisk broom	4%	38.457	0.352	0.992	6.607
Uniform whisk broom	1%	36.290	0.416	0.990	8.881
Guided whisk broom	1%	36.597	0.413	0.989	7.853

References

1. F. Yasuma, T. Mitsunaga, D. Iso, and S. K. Nayar, “Generalized Assorted Pixel Camera: Postcapture Control of Resolution, Dynamic Range, and Spectrum,” IEEE Transactions on Image Processing 19(9), 2241–2253 (2010).
2. A. Chakrabarti and T. Zickler, “Statistics of real-world hyperspectral images,” in CVPR 2011 (2011), pp. 193–200.
3. B. Arad and O. Ben-Shahar, “Sparse Recovery of Hyperspectral Signal from Natural RGB Images,” in European Conference on Computer Vision (Springer, 2016), pp. 19–34.
4. I. Choi, D. S. Jeon, G. Nam, D. Gutierrez, and M. H. Kim, "High-Quality Hyperspectral Reconstruction Using a Spectral Prior," ACM Transactions on Graphics (Proc. SIGGRAPH Asia 2017) 36(6), 218:1–13 (2017).
5. X. Cao, X. Tong, Q. Dai, and S. Lin, "High resolution multispectral video capture with a hybrid camera system," in CVPR 2011 (2011), pp. 297–304.
6. V. Saragadam and A. C. Sankaranarayanan, “KRISM—Krylov Subspace-based Optical Computing of Hyperspectral Images,” ACM Trans. Graph. 38(5), 1–14 (2019).